

A Semantic SLAM Model for Autonomous Mobile Robots Using Content Based Image Retrieval Techniques

Choon Ling Tan*, Simon Egerton*, and Velappa Ganapathy*

Monash University, Jalan Lagoon Selatan,
Bandar Sunway, 46150, Selangor Darul Ehsan,
Malaysia
cltan4@student.monash.edu,
simon.egerton@infotech.monash.edu.my,
velappa.ganapathy@eng.monash.edu.my
<http://www.monash.edu.my>

Abstract. Semantic approaches to conducting SLAM are still considered to be comparatively new compared to other methods. To this end, we introduce a new model for conducting SLAM on an autonomous mobile robot equipped with vision sensors. Our model consists of four separate stages, each with a specific goal at hand, namely: feature extraction, classification and storage, semantic analysis, and location resolving. This is the first time SLAM has been examined in this way and a set of planned experiments and benchmarks are also discussed which apply the proposed model to environments which are unknown and vary in their structure. Initial experiments are also included where images captured in different indoor locations are shown, along with the similarity scores of these images. Future work and experiments that are intended to be completed are then discussed.

Keywords: image patch, image segment, image signature, semantic SLAM, CBIR, Tamura texture.

1 Introduction

The problem of Simultaneous Localization and Mapping (SLAM) can be described as a situation where an autonomous robot – equipped with one or more low-level sensors – is placed within an unknown environment and is required to perform two tasks simultaneously: the first is known as localization where the robot estimates its current location in the environment relative to other “visible” objects, whereas the second is called mapping, where the robot records its own position in addition to any objects and obstacles within the current environment.

Having its origins from [20] where the issue of representing spatial information during the application of robotics is brought up, many traditional methods of conducting SLAM have been developed over the years. Such methods include those from Thrun [9], [22], [23], Davison [3], [19], and Little [6], [7]. While such methods of

* Choon Ling Tan and Simon Egerton are currently attached to the School of Information Technology, and Velappa Ganapathy is currently attached to the School of Engineering.

SLAM possess different implementations, they have the common feature of tracking topological information on a geometric level.

However, there have been several research efforts recently that have focused upon conducting SLAM on a semantic level [4], [8], [16] where high-level information is inferred from regular topological maps as suggested in [4]. This allows a greater amount of information pertaining to the environment (i.e. such as the navigability or the nature of certain areas) to be recorded, in addition to representing the presence of obstacles. For instance, in [17], certain occupied cells within an occupancy grid are labeled to indicate the presence of buildings, whereas in [18] and [8], certain regions of the map are classified according to different key objects that have been tracked.

Research into the field of semantic mapping is considered to be new. There are few papers that have been published regarding the subject and the majority of them are very recent. It is in the interest of contributing towards this field that we propose conducting semantic SLAM though content-based image retrieval (CBIR). Implementing CBIR to achieve a semantic form of SLAM is new in itself and provides advantages over traditional feature-based methods. For example, the semantic information has the potential to be queried by a human using natural language. Moreover, we believe such semantic methods have tenable biological parallels.

2 Model

We propose an approach of handling the SLAM problem by implementing CBIR with the aid of cameras. As seen in Fig. 1., the proposed model consists of four separate stages: (1) feature extraction, (2) classification and storage, (3) semantic analysis, and (4) location resolving. Each stage is composed of various sub-stages that contribute towards the overall goal of the stage. A description of each stage will be explained below.

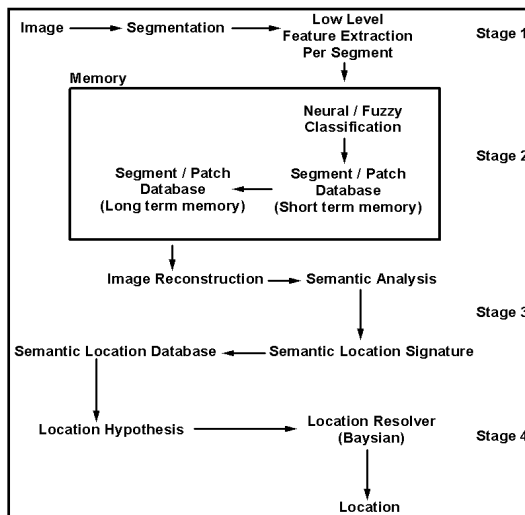


Fig. 1. The various stages within the proposed model

2.1 Stage 1 (Feature Extraction)

This stage begins with obtaining an image of the surrounding environment as input from vision sensors. This image is then segmented into 40 equally-sized portions, of which the process of feature extraction is conducted on each segment, or patch. The feature extraction in this last sub-stage is similar to that in [11] and [13] where the low-level Tamura texture features of coarseness, contrast and directionality [21] [1] are extracted as [12] has indicated the potential of implementing such features within the context of CBIR. In the event that such features prove to be inadequate in allowing sufficient variation in the latter stages of semantic analysis within the model, we will revise this stage accordingly to implement other features suitable to CBIR as documented in [5].

The features of coarseness, contrast and directionality are calculated by applying a procedure that is similar to the one implemented by [20], the following steps are performed to determine the coarseness value of a particular patch:

Step 1: For each pixel point (x, y) within the image patch, calculate the sum total over neighbourhoods where the sizes are powers of two (i.e. $1 * 1, 2 * 2, \dots, 32 * 32$). The sum total over the size 2^k neighbourhood at point (x, y) is

$$\text{Sum}_{k,v}(x, y) = \sum_{i=x-2^{k-1}+1}^{x+2^{k-1}} \sum_{j=y}^{y+2^{k-1}-1} f(i, j) \quad (1)$$

for the vertical orientation, v , and

$$\text{Sum}_{k,h}(x, y) = \sum_{i=x-2^{k-1}+1}^x \sum_{j=y-2^{k-1}+1}^{y+2^{k-1}-1} f(i, j) \quad (2)$$

for the horizontal orientation, h , where $f(i, j)$ is the gray-level pixel value at (x, y) .

Step 2: For each and every pixel point of each value of k , calculate the differences between the sum total corresponding to pairs of non-overlapping, equal sized neighbourhoods in both vertical and horizontal orientations, where:

$$E_{k,v}(x, y) = (\text{Sum}_{k,v}(x, y) - \text{Sum}_{k,v}(x, y - 2^k)) / 2^{2k} \quad (3)$$

for the vertical orientation, v , and

$$E_{k,h}(x, y) = (\text{Sum}_{k,h}(x, y) - \text{Sum}_{k,h}(x + 2^k, y)) / 2^{2k} \quad (4)$$

for the horizontal orientation, h .

Step 3: For each and every pixel point, analyse the output values as a result from the previous step, and select the best size, k , that gives the highest value:

$$S_{\text{best}}(x, y) = 2^k \quad (5)$$

where k maximizes E in either orientation:

$$E_{\text{max}} = \max (E_{1, h}, E_{1, v}, E_{2, h}, E_{2, v} \dots, E_{5, h}, E_{5, v}) \quad (6)$$

Step 4: Finally, calculate the coarseness measure of the entire image patch by averaging all S_{best} values:

$$F_{\text{crs}} = \frac{1}{m \cdot n} \sum_{i=0}^m \sum_{j=0}^n S_{\text{best}}(i, j) \quad (7)$$

where m and n are the width and height of the image patch, respectively.

The method of measuring the value of contrast for any particular image patch is also explained in [20] with the following steps are performed:

Step 1: For each image patch, obtain a histogram of gray-level differences in order to, calculate the average gray-level value:

$$\text{Avg}_{\text{image}} = \text{sum}(\sum_{i=1}^{256} \text{bin}(i) * \frac{\text{count}(i)}{m \cdot n}) \quad (8)$$

where $\text{bin}(i)$ is the i^{th} bin value with a histogram count of $\text{count}(i)$, and m and n are the width and height of the image patch, respectively.

Step 2: Calculate the fourth moment about the mean, μ_4 with the following equation:

$$\mu_4 = \text{sum}((\sum_{i=1}^{256} \text{bin}(i) - \text{Avg}_{\text{image}})^4 * \frac{\text{count}(i)}{m \cdot n}) \quad (9)$$

Step 3: Measure the amount of polarization by defining the kurtosis, α_4 as

$$\alpha_4 = \mu_4 / \sigma^4 \quad (10)$$

where σ^2 is the variance, which is calculated as

$$\sigma^2 = \text{sum}((\sum_{i=1}^{256} \text{bin}(i) - \text{Avg}_{\text{image}})^2 * \frac{\text{count}(i)}{m \cdot n}) \quad (11)$$

Step 4: Finally, combine σ and α_4 to obtain the contrast measure with the equation

$$F_{\text{con}} = \sigma / \alpha_4^{0.25} \quad (12)$$

[20] also provides the method of calculating the feature of directionality in which we implement as explained in the following steps:

Step 1: declare the following two 3×3 operators to aid in calculating the horizontal and vertical differences, ΔH and ΔV respectively, where

$$\text{OP}_H = \begin{bmatrix} -1 & 0 & 1 \\ -1 & 0 & 1 \\ -1 & 0 & 1 \end{bmatrix} \quad \text{OP}_V = \begin{bmatrix} 1 & 1 & 1 \\ 0 & 0 & 0 \\ -1 & -1 & -1 \end{bmatrix}$$

Step 2: Calculate ΔH and ΔV for each gray-level pixel point $f(i, j)$ in the image patch, where each 3×3 size neighbourhood with $f(i, j)$ in the centre is multiplied with either OP_H , or OP_V , depending on the orientation, and then taking the sum total. These calculations for ΔH and ΔV can be summarized as:

$$\Delta H(x, y) = \text{sum}(\sum_{i=x-1}^{x+1} \sum_{j=y-1}^{y+1} f(i, j) * \text{OP}_H) \quad (13)$$

$$\Delta V(x, y) = \text{sum}(\sum_{i=x-1}^{x+1} \sum_{j=y-1}^{y+1} f(i, j) * \text{OP}_V) \quad (14)$$

Step 3: From ΔH and ΔV , we are able to obtain a magnitude ΔG , where

$$\Delta G = (|\Delta H| + |\Delta V|) / 2 \quad (15)$$

and the local edge direction for each pixel point, $\theta(i, j)$, where

$$\theta(i, j) = \begin{cases} 0 & \text{iff } \Delta_H(i, j) = 0 \text{ and } \Delta_V(i, j) = 0 \\ \pi & \text{iff } \Delta_H(i, j) = 0 \text{ and } \Delta_V(i, j) > 0 \\ \tan^{-1}(\Delta_V(i, j) / \Delta_H(i, j)) + \frac{\pi}{2} & \text{otherwise} \end{cases} \quad (16)$$

Step 4: Obtain the histogram HD by quantizing θ over bin values that range from 0 to π , as shown by an example in Figure 3. Following that, we apply a threshold process on to HD where any bin with a count value < 0.01 will have its respective count value be reset to 0. This is done in order to filter out the counting of unreliable directions that cannot be considered as edge points.

Step 5: The directionality is finally determined by calculating the sharpness of the peaks in HD . This is done by summing the peaks across the entire histogram, thusly:

| | |
|--|------|
| $\text{Fdir} = \text{Fdir} + \sum_{m=1}^{\text{length}(HD)} (\phi_m - \phi_p * 0.0001)^2 * H_D(m)$ | (17) |
|--|------|

where ϕ_m is the value of the m^{th} bin, ϕ_p is the bin value of the highest count (peak) within the histogram, and $H_D(m)$ is the count value of the m^{th} bin.

From these features, a feature vector that is able to uniquely identify each patch is constructed, this is also known as an patch signature, and the 40 patch signatures within a single image constitute as a single image signature (shown in Fig. 2.), which is similar in concept to shape signatures used in [24]. Image signatures are required in

order to provide some sort of semantic context to the location in which each batch of image patches was captured. This is done by comparing semantic descriptions that are extracted from the image signatures. Direct comparison between two sets of image signatures is not done; as it is possible that two similar images can generate different image signatures due to background noise (such as new objects appearing within the scene). Under such circumstances, comparison between image signatures would fail under typical fuzzy or Euclidean distance measures.

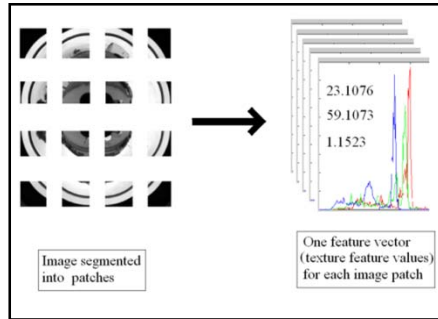


Fig. 2. Construction of an image signature

It is expected that by extracting semantic information, a match would be able to be produced, as new objects introduced in the scene may result in a different group of patches, but the unaffected patches will still be able to produce a semantic description that closely resembles its counterpart from the other image (without the offending object), and hence, generate a match.

From the fuzzy model of [13] and the variable weight assignment model as implemented by [14], it is suggested that matching high-level concepts between images is possible, but as with most CBIR techniques, relies on training before achieving a high success rate.

The Tamura texture features (i.e. coarseness, contrast, and directionality) which are extracted from each image patch have a single floating-point value attached to each of the features, which are calculated by applying a procedure that is similar to the one implemented by [21].

2.2 Stage 2 (Classification and Storage)

After the process of constructing patch signatures is completed, they are then presented to a fuzzy/neural network classifier, or some other appropriate self-organizing network. This is an important factor to consider, as the classifier should not be limited to a fixed number of classes, but grow accordingly instead as the variance in signatures demands an increasing number of classes.

Each class is determined by a <patch signature, patch> pairing, which is required during image reconstruction in the next stage. Note that a graphical, visual reconstruction of images is not necessary at this development stage, as the proposed semantic analysis would work equally as well on class labels generated from the

self-organizing neural network. Such an action may still prove to be useful in later developments in order to aid in enhancing semantic descriptions (i.e. using object recognition or further CBIR techniques).

Thus, the classifier acts as the short-term memory portion of this stage, while $\langle \text{patch signature}, \text{patch} \rangle$ pairs being copied into long-term memory whenever a semantic description uses that pairing. However, it is possible for the classifier to generate classes that will never be used. Through this method, a robot traversing through an environment will classify captured images according to Fig. 3.

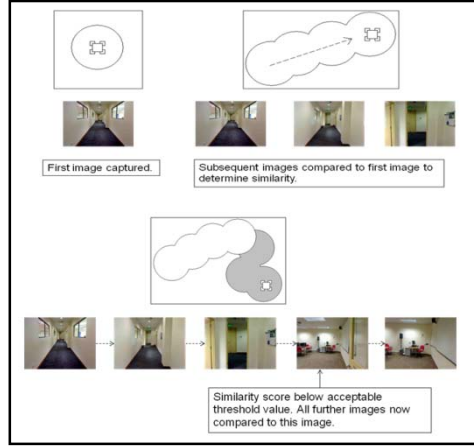


Fig. 3. Classification of images

The input variables consist of the three Tamura texture features of coarseness, contrast and directionality, each with 2 trapezoidal-shaped membership functions. A single output variable with 2 trapezoidal-shaped membership functions is determined after the input variables are processed through a fuzzy rule set in order to determine the final similarity score of any particular image. This can be seen in Fig. 4. below.

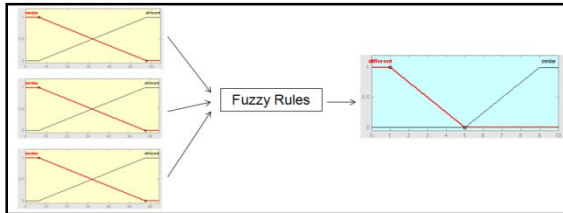


Fig. 4. Input/Output variables of the fuzzy inference system

The fuzzy rule set currently consists of 6 rules where each input variable-membership function tuple is mapped to the corresponding membership function in the output variable, as seen in Fig. 5.

| |
|--|
| 1. If (coarseness is similar) then (similarity is similar) (1) |
| 2. If (contrast is similar) then (similarity is similar) (1) |
| 3. If (directionality is similar) then (similarity is similar) (1) |
| 4. If (coarseness is different) then (similarity is different) (1) |
| 5. If (contrast is different) then (similarity is different) (1) |
| 6. If (directionality is different) then (similarity is different) (1) |

Fig. 5. Fuzzy rules of the inference system

2.3 Stage 3 (Semantic Analysis)

Once patch signatures have been classified into various groups, each and every captured image is to be reconstructed through the use of only the unique patch signatures that have been stored within the database. Following this, reconstituted images are then analyzed in order to determine the relationship between image patches. Each cluster of patches that are within the same classification is given labels denoting the semantic relationship with other patch clusters as well as its current location within the entire image. This can be seen in Fig. 6, where the patch cluster of C1 is to the left of the patch cluster of C2.

| | | | | | |
|--|----|----|----|--|--|
| | C1 | C1 | C2 | | |
| | C1 | C1 | C2 | | |
| | | | C2 | | |
| | | | C2 | | |
| | | | | | |
| | | | | | |

Fig. 6. Relative locations between patch clusters

Therefore, the cluster of C1 is to be annotated with the relationship labels of:

Right(C1) = C2
Location(C1) = top left

In order to provide a certain degree of flexibility in regards to relationships between clusters, we attach high-level descriptors to them, rather than noting the specific patch indices that constitute a cluster. For instance, if cluster C1 were to shift left, the labels denoting the relationship between C1 and C2 would still hold, whereas that might not necessarily be true if specific patch indices were recorded.

The aggregate of all labels related to one cluster is considered to be the semantic location signature for that cluster. There also exists the possibility of detecting high-level features that are present within the captured images such as object recognition [18] to further contribute towards the amount of semantic data present within each semantic location signature.

As an example, consider the image in Fig. 7(a), which has 5 potential semantic areas of interest that can be treated as classes. These areas are divided within the regions as shown in Fig. 7(b) where C1 to C5 are the counter, ceiling, door,

wall/railing, and floor, respectively. Therefore, the reconstituted counterpart to this image would be as seen in Fig. 7(c) in the next page.

The semantic descriptions for each and every cluster (and hence, the entire reconstructed image) is then entered into a semantic descriptor database. This database is responsible for comparing existing descriptors within in against their incoming counterparts to determine if a match is possible. Towards this end, a semantic reasoning system with an implementation similar to that of [2] with Research Cyc as the knowledge base of choice.

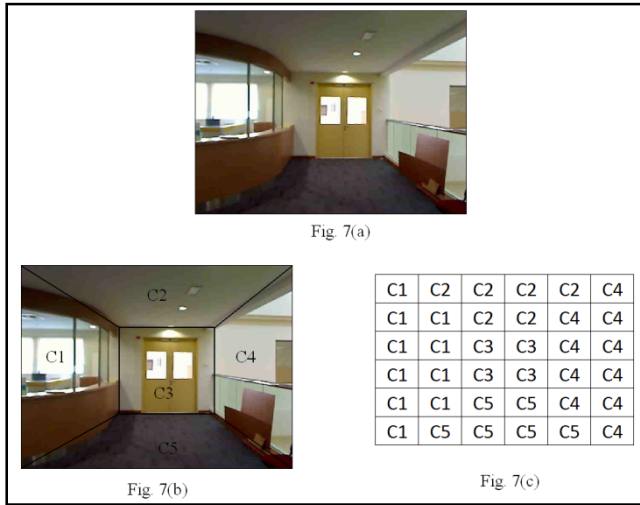


Fig. 7. Reconstruction of an image

2.4 Stage 4 (Location Resolving)

As a result of the previous stage, a set of location hypothesis (i.e. a set of locations each labeled with a probability) is generated. Such sets are generally caused by noise and perceptual aliasing (a situation where different locations appear similar to each other). Therefore, this final stage of resolving which location the robot is currently at is required, as simply selecting the location with the highest probability is naïve.

Bayesian reasoning opens up the possibility of determining the most likely location the robot is currently at by considering where the robot assumes its current location is, along with a new set of location hypothesis. However, a common problem that arises from this is method is the issue of location, or orientation independence. As an example, it can be difficult to recognize that a previous location has been revisited as it was viewed from a significantly different angle. One solution towards this problem is to implement a panoramic image sensor, which can be financially prohibitive and not easily available. Therefore, we attempt to overcome the aforementioned issue through another method, where locations are semantically related to each other by tracking either unique patches, or a unique ordering of patches.

3 Experiments

Three preliminary experiments have already been conducted in the MATLAB environment, where images with a resolution of $640 * 480$ pixels are segmented in a similar manner to that in [10]. However, in order to obtain a meaningful amount of semantic data, each image patch consists of $96 * 80$ pixels, resulting in 40 separate image patches per image. The size of image patches is determined through the use of the `bestblk` command within the MATLAB environment, which specifies the optimal patch size for processing.

The results of our experiments are shown in Fig. 8., where the 20th patch of 3 separate images are analyzed and their respective color and texture features are extracted. It is expected that the differences between image patches of separate images (i.e. as a result of their feature comparisons) can be transposed to a higher, semantic level, which also implies differences between entire images, as an entire image can be said to be a larger version of an image patch with its signature composed of multiple, smaller sub-signatures.

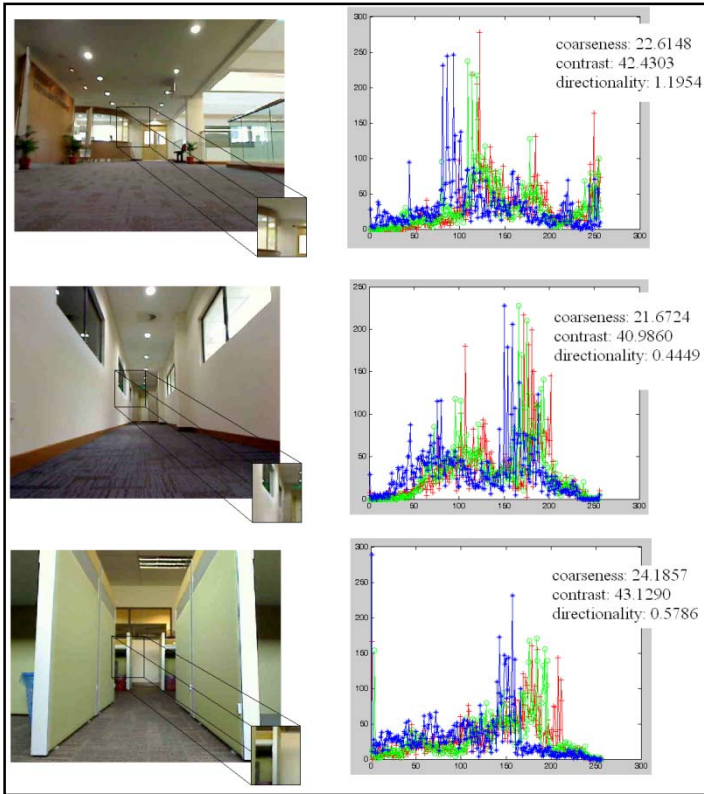


Fig. 8. Images of an open concourse area (top), a corridor (middle), and a cubicle room (bottom), with the extracted feature information of the indicated image patch region

These results appear to be encouraging. While the color histograms for each image patch have a unique distribution curve, there is also the possibility that the Tamura texture feature values also tend to favor a specific image-location pairing, with each image possessing a specific feature value that is distinct from the others. In this case, the image patch for the open concourse area has a high directionality compared to the others, while the cubicle room image patch has a somewhat higher coarseness.

Following this, the next experiment applies the fuzzy logic system from [15] on to the image signature vector to determine if Tamura textures alone are able to detect differences between images in the same capacity as RGB histograms. Experiments with the RGB histogram and Tamura texture feature components were conducted to

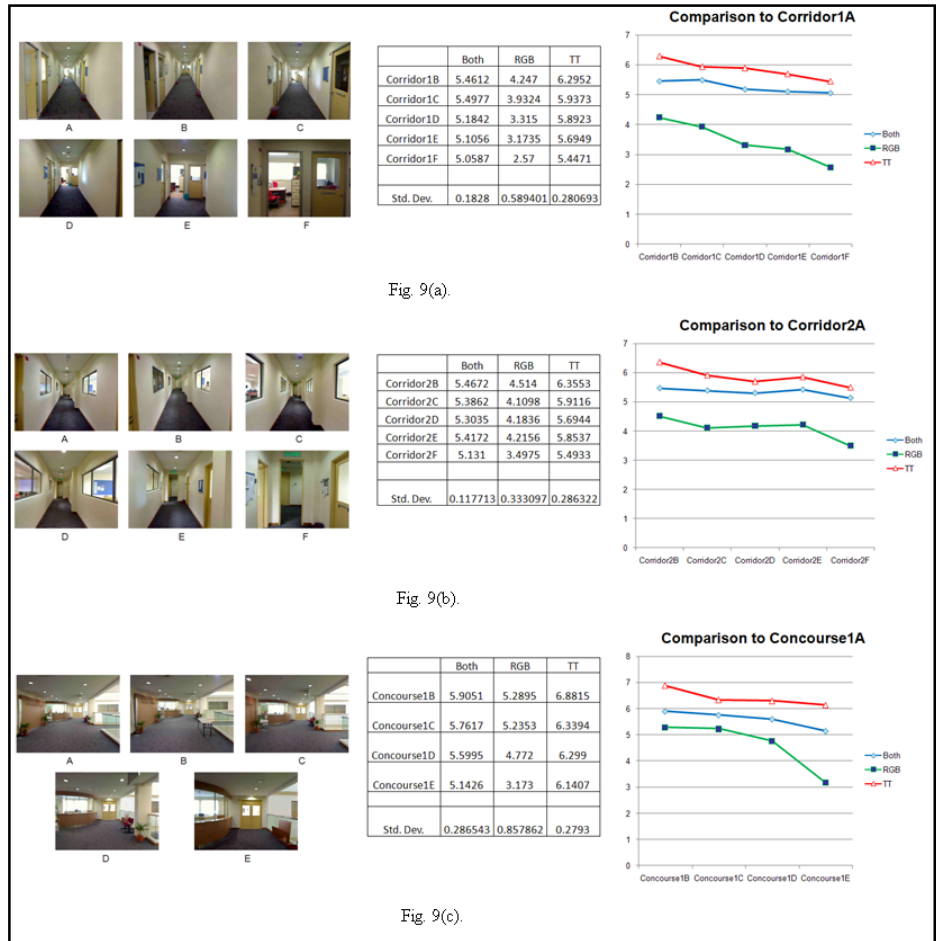


Fig. 9(a).

Fig. 9(b).

Fig. 9(c).

Fig. 9. The image sets of Corridor1 (a), Corridor 2 (b) and Concourse (c), with their respective results

determine the degree of influence of each image signature component in fuzzy logic classification. Data for this experiment consists of 3 separate locations, 2 corridor sets and 1 concourse set, which can be seen in Fig. 9. The compiled results indicate a high possibility that Tamura texture features alone are able to be implemented in the proposed model. With only one exception (Corridor2E), the values of all image signatures follow a decreasing trend as the robot traverses the various environments selected for the experiment.

The goal of the final experiment is to determine the similarity score value which indicates a change in area (i.e. from a corridor to a room) during the classification process. To this end, 4 separate image sequences have been recorded, each consisting of 2 separate areas. The results are shown in Fig. 10., where the shaded letters indicate that the location of that image is semantically different than its predecessors (i.e. in Fig. 10(a), image A – J consists of a corridor area, whereas K – M consists of a room area). These results indicate that threshold value in similarity is around roughly 5.37 – 5.65. However, there have been several instances where images belonging within the same area have values below this threshold, such as in images H – J in Fig. 10(a). Therefore, further refinement towards the model is required before attempting to proceed into further stages within the proposed model.

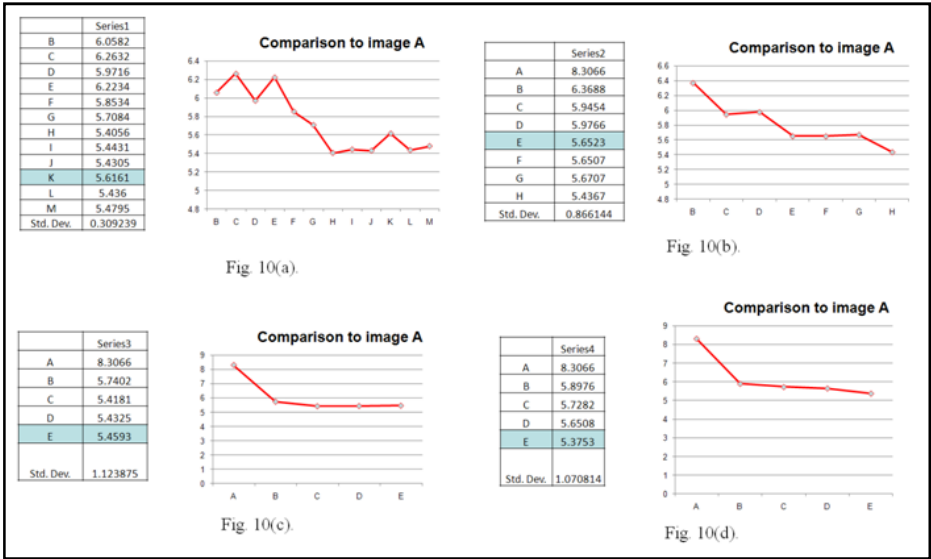


Fig. 9. Results for dual-area experiments

4 Conclusion

In this paper, we have presented a semantic based SLAM model. This model is based on four separate stages with the goals of feature extraction, classification and storage, semantic analysis, and location resolving. We also describe three preliminary

experiments which demonstrate that implementation of Tamura texture features (i.e. coarseness, contrast, and directionality) alone are capable of producing noticeable differences in similarity scores when supplied with a series of images as a mobile robot traverses an environment. While further development is required for Stages 3 and 4 of the proposed model, we see our model as potential contribution towards semantic, and especially ontologically based methods that play a key role in future developments of both SLAM and generalized mapping models.

References

1. Chiu, C.Y., Lin, H.C., Yang, S.N.: A Fuzzy Logic CBIR System. In: 12th IEEE International Conference on Fuzzy Systems, FUZZ 2003, May 28, vol. 2, pp. 1171–1176 (2003)
2. Daoutis, M., Coradeschi, S., Loutfi, A.: Integrating Common Sense in Physically Embedded Intelligent Systems. In: Proceedings of the 5th International Conference on Intelligent Environments, vol. 2, pp. 212–219 (2009)
3. Davison, A.: Real-Time Simultaneous Localization and Mapping with a Single Camera. In: Proceedings of the Ninth International Conference on Computer Vision ICCV 2003, Nice, France, pp. 1403–1410 (2003)
4. Dellaert, F., Bruemmer, D.: Semantic SLAM for Collaborative Cognitive Workspaces. In: Presented at the AAAI Fall Symposium Series, Arlington, VA, USA (2004)
5. Deselaers, T., Keyzers, D., Ney, K.: Features for Image Retrieval: An Experimental Comparison. *Information Retrieval* 11(2), 77–107 (2008)
6. Elinas, P., Little, J.J.: Stereo Vision SLAM: Near Real-Time Learning of 3D Point-Landmark and 2D Occupancy-Grid Maps Using Particle Filters. In: 2007 IEEE/RSJ International Conference on Intelligent Robots and Systems, IROS 2007 (2007) (to be published)
7. Elinas, P., Sim, R., Little, J.J.: SLAM: Stereo Vision SLAM Using the Rao-Blackwellised Particle Filter and a Novel Mixture Proposal Distribution. In: Proc. 2006 IEEE International Conference on Robotics and Automation (ICRA 2006), pp. 1564–1570 (2006)
8. Galindo, C., Saffiotti, A., Coradeschi, S., Buschka, P., Fernandez-Madrigal, J., Gonzalez, J.: Multi-hierarchical Semantic Maps For Mobile Robotics. In: Proc. of the IEEE/RSJ Intl. Conf. on Intelligent Robots and Systems (IROS 2005), Edmonton, CA, USA, pp. 3492–3497 (2005)
9. Hahnel, D., Thrun, S., Wegbreit, B., Burgard, W.: Towards Lazy Data Association in SLAM. In: Proceedings of the 11th International Symposium of Robotics Research (ISRR 2003), Sienna, Italy (2003)
10. Jhanwar, N., Chaudhuri, S., Seetharaman, G., Zavidovique, B.: Content Based Image Retrieval Using Motif Cooccurrence Matrix. *Image and Vision Computing* 22(14), 1211–1220 (2004)
11. Jonsgård, O.A.F.: Improvements on Colour Histogram-based CBIR. Gjøvik University College, Norway (2005)
12. Kulkarni, S., Verma, B.: Fuzzy Logic based Texture Queries for CBIR. In: Fifth International Conference on Computational Intelligence and Multimedia Applications (ICCIMA 2003), pp. 223–228 (2003)
13. Lakdashti, A., Moin, M.S., Badie, K.: Semantic-Based Image Retrieval: A Fuzzy Modeling Approach. In: IEEE/ACS International Conference on Computer Systems and Applications (AICCSA 2008), Doha, Qatar, pp. 575–581 (2008)

14. Liu, P., Jia, K., Wang, Z., Lv, Z.: A New And Effective Image Retrieval Method Based On Combined Features. In: Fourth International Conference on Image and Graphics (ICIG 2007), Sichuan, China, pp. 786–790 (2007)
15. Mouragnon, E., Lhuillier, M., Dhome, M., Dekeyser, F., Sayd, P.: Monocular Vision Based SLAM for Mobile Robots. In: Proceedings of the 18th International Conference on Pattern Recognition, vol. 3, pp. 1027–1031 (2006)
16. Nuchter, A., Surmann, H., Lingemann, K., Hertzberg, J.: Semantic Scene Analysis Of Scanned 3D Indoor Environments. In: Proceedings of the 8th International Fall Workshop Vision, Modeling, and Visualization 2003 (VMV 2003), Munich, Germany, pp. 215–222 (2003)
17. Persson, M., Duckett, T., Valgren, C., Lilienthal, A.: Probabilistic Semantic Mapping with a Virtual Sensor for Building Nature Detection. In: Proc. IEEE Int. Symp. on Computational Intelligence in Robotics and Automation (CIRA 2007), pp. 236–242 (2007)
18. Rottmann, A., Mozoz, O.M., Stachniss, C., Burgard, W.: Semantic Place Classification of Indoor Environments with Mobile Robots using Boosting. In: Proc. Nat. Conf. Artif. Intell (AAAI), pp. 1306–1311 (2005)
19. Smith, P., Reid, I., Davison, A.: Real-Time Monocular SLAM with Straight Lines. In: British Machine Vision Conference, vol. 1, pp. 17–26 (2006)
20. Smith, R., Self, M., Cheeseman, P.: Estimating Uncertain Spatial Relationships in Robotics. In: Autonomous Robot Vehicles, pp. 167–193. Springer, Heidelberg (1990)
21. Tamura, H., Mori, S., Yamawaki, T.: Textural Features Corresponding to Visual Perception. *IEEE Transactions on Systems, Man and Cybernetics* 8(6), 460–473 (1978)
22. Thrun, S.: Robotic Mapping A Survey. In: Exploring Artificial Intelligence in the New Millenium. Morgan Kaufmann, San Francisco (2002)
23. Thrun, S., Thayer, S., Whittaker, W., Baker, C., Burgard, W., Ferguson, D., Hahnel, D., Montemerlo, D., Morris, A., Omohundro, Z., Reverte, C., Whittaker, W.: Autonomous Exploration and Mapping of Abandoned Mines. *IEEE Robotics and Automation Magazine* 11(4), 79–91 (2004)
24. Zhang, D., Lu, G.: A Comparative Study on Shape Retrieval Using Fourier Descriptors with Different Shape Signatures. In: Proc. of International Conference on Intelligent Multimedia and Distance Education (ICIMADE 2001), Fargo, ND, USA, June 1, pp. 1–9 (2001)